2013 IEEE/ASME International Conference on
Advanced Intelligent Mechatronics (AIM)
Wollongong, Australia, July 9-12, 2013

Improving Dynamic Performance of Bi-articularly Actuated Robot Arms by Using Infinity Norm Based Actuation Redundancy Resolution

Valerio Salvucci[1] and Takafumi Koseki[1]

Abstract— **Bi-articular actuators, actuators spanning two joints, are gaining popularity for solving the known limitations of conventional robot arms. Actuator redundancy resulting from the presence of bi-articular actuators increases stability, transfers mechanical energy from proximal to distal joints, and decreases the non-linearity of the end effector force as a function of force direction. In this paper, advantages of infinity norm optimization criteria for actuator redundancy resolution of bi-artiularly actuated robot arms is investigated under dynamic conditions. The infinity norm approach with closed form solution is compared with the pseudo inverse matrix based methods by simulation means. When using the infinity norm based approach, under the same robot arm dynamics, the required maximum joint actuator is reduced; and under the same joint actuator limitations the achievable maximum end effector acceleration is increased.**

I. INTRODUCTION

Robot arms presenting animal musculo-skeletal characteristics such as bi-articular actuators — actuators that span two joints — have been proposed for more than two decades [1] due to the numerous advantages they yield.

First, bi-articular actuators dramatically increase the range of end effector impedance which can be achieved without feedback [1]. Consequences are, for example, the capability of path tracking and disturbance rejection using just feedforward control [2], and improvement of balance control for legged robots without force sensors [3]. Second, bi-articular actuators transfer mechanical energy from proximal to distal joints [4]. This is a key aspect in legged robots for hopping [5], [6], for jumping [7], for running [8], [9], and for disturbance rejection [10]. In addition, bi-articularly actuated manipulators produce a maximum output force at the end effector in a more homogeneous distributed way [11].

Regarding the hardware design, bi-articularly actuated robots have been realized by means of linear actuators [5], [8], [12], and motors with transmissions systems based on pulleys [13], [14], planetary gears, [15], [16], wires [17], [18], and passive springs [19].

From a control point of view, bi-articularly actuated robots often present more actuators than joints, resulting in actuator redundancy. The resolution of actuator redundancy represents a key point in the control design for such robots.

Pseudo-inverse matrices are often used for actuator redundancy resolution [14], [20]. Moore-Penrose is the simplest pseudo-inverse matrix, and correspond to the minimization of the 2 norm [21].

In our previous work [22] we proposed a new approach based on a closed form expression minimizing the infinity norm to resolve actuator redundancy for bi-articularly actuated robot arms, and experimentally verified it [23]. The infinity norm based approach has been compared to the traditional 2 norm based approach under static conditions.

In this work, we compare the traditional 2 norm based approach for actuator redundancy resolution with the infinity norm approach under dynamic conditions. The analysis is carried out by simulating a two-link robot arm actuated by one bi- and two mono articular actuators. Factors such as actuator joint torques and end effector acceleration are investigated.

Modeling of bi-articularly actuated robot arms is shown in section II. In section III and section IV, the redundancy actuator problem and the resolution approaches based on 2 norm and infinity norm are described. In section V the simulation details are illustrated. In section VI, the resulting actuator joint torques and end effector acceleration are shown, and analyzed in section VII. Finally, in section VIII, the advantages of the infinity norm approach are summarized.

II. MODELING OF BI-ARTICULARLY ACTUATED ROBOT ARMS

In conventional robot arms each joint is driven by one actuator. On the other hand, animal and human limbs present a complex musculo-skeletal structure based on mono- and multi- articular muscles. Mono-articular muscles produce a torque about one joint. Multi-articular muscles span more than one joint. A widely used simplified model of the complex animal musculo-skeletal system [13], [24], [25], [23], [26], [27], [28], is shown in Fig. 1. This model is based on six contractile actuators — three extensors (e1, e2, and e3) and three flexors (f1, f2, and f3) — coupled in three antagonistic pairs:

- e1–f1 and e2–f2: couples of mono-articular actuators producing torques about joint 1 and 2, respectively.
- e3–f3: couple of bi-articular actuators producing torque about joint 1 and 2 at the same time.

The resulting forces at the end effector are shown in Fig. 1. If only mono-articular muscles are considered, there are four resulting forces at the end effector and the maximum output force space is a quadrilateral. On the other hand, if bi-articular actuators are added, there are six forces at the end effector, hence the maximum output force space becomes an hexagon.

[1]V. Salvucci and T. Koseki are with Department of Electrical Engineering and Information System, The University of Tokyo, 3–7–1 Hongo, Bunkyoku, Tokyo, 113–8656, Japan valerio at koseki.t.u-tokyo.ac.jp, takafumikoseki at ieee.org

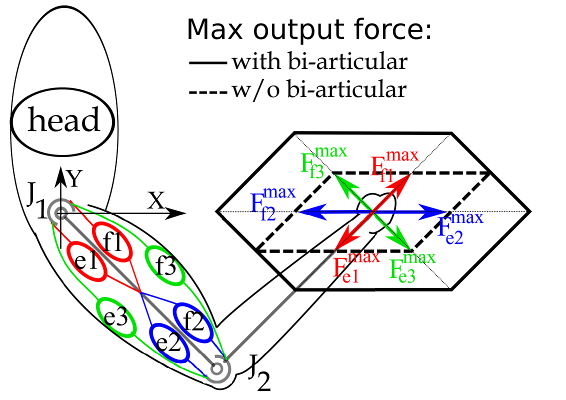

Fig. 1. Two-link arm with four mono- and two bi-articular actuators: model and resulting forces at the end effector

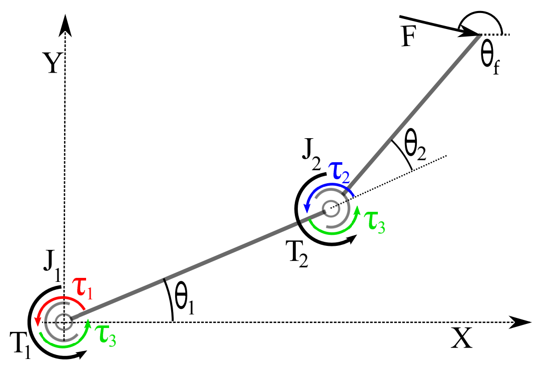

Fig. 2. Statics of two-link arm with four mono- and two bi-articular actuators

III. ACTUATOR REDUNDANCY PROBLEM

The resulting statics of the bi-articularly actuated arm of Fig. 1 are shown in Fig. 2, where:

- The total torques about joint 1 and 2 are T_1 and T_2, respectively ($\boldsymbol{T} = [T_1, T_2]^T$.
- The torques produced by mono-articular actuators about joints 1 and 2 are τ_1 and τ_2, respectively. They are calculated from the actuator input forces e_i and f_i for $i = (1,2)$ as:

$$\tau_1 = (f_1 - e_1)r \tag{1}$$

$$\tau_2 = (f_2 - e_2)r \tag{2}$$

  where r is the distance between the joint axis and the point where the muscle force is applied. The value of r is consider to be the same for all the muscles and all joint angles.
- The bi-articular torque produced about both joints is τ_3:

$$\tau_3 = (f_3 - e_3)r \tag{3}$$

- $\boldsymbol{F}$ is a general force at the end effector with magnitude F and direction θ_f.

The statics of this system are expressed by:

$$\begin{bmatrix} T_1 \\ T_2 \end{bmatrix} = J^T \begin{bmatrix} F_x \\ F_y \end{bmatrix} \tag{4}$$

where J is the robot arm Jacobian, F_x and F_y are the orthogonal projection of $\boldsymbol{F}$ on the x-axis and y-axis, respectively. A two-link manipulator with the statics shown in Fig. 2 presents actuator redundancy:

$$\boldsymbol{T}^T = \boldsymbol{B}\boldsymbol{\tau}^T = \begin{bmatrix} 1 & 0 & 1 \\ 0 & 1 & 1 \end{bmatrix} \begin{bmatrix} \tau_1 \\ \tau_2 \\ \tau_3 \end{bmatrix} \tag{5}$$

Given τ_1, τ_2, and τ_3, it is possible to determine $\boldsymbol{T}$, and therefore $\boldsymbol{F}$ by using (4). On the other hand, given $\boldsymbol{F}$, and therefore $\boldsymbol{T}$, it is generally not possible to determine uniquely $\boldsymbol{\tau}$ due to the actuator redundancy. The problem represented by (5) is referred to as the redundancy actuator problem in the following.

IV. 2 AND INFINITY NORM APPROACHES FOR ACTUATOR REDUNDANCY RESOLUTION

Given the arm with the statics as in Fig. 2 and a desired force at the end effector $\boldsymbol{F}$, the desired joint torques $\boldsymbol{T}$ are calculated using (4), and the three desired joint actuator torques τ_1, τ_2, and τ_3 producing $\boldsymbol{T}$ are calculated using the 2 norm and the infinity norm approaches as described in Section IV-A and Section IV-B, respectively.

A. 2 norm based approach

The actuator redundancy is resolved using the 2 norm by solving the following problem:

$$\begin{array}{ll} \min & \sqrt{(\tau_1)^2 + (\tau_2)^2 + (\tau_3)^2} \\ \text{s.t.} & T_1 = \tau_1 + \tau_3 \\ & T_2 = \tau_2 + \tau_3 \end{array} \tag{6}$$

The solution of the problem expressed by (6) is [23]:

$$\tau_1 = \frac{2}{3}T_1 - \frac{1}{3}T_2 \tag{7}$$

$$\tau_2 = -\frac{1}{3}T_1 + \frac{2}{3}T_2 \tag{8}$$

$$\tau_3 = \frac{1}{3}T_1 + \frac{1}{3}T_2 \tag{9}$$

B. Infinity norm based approach

The actuator redundancy is resolved using the infinity norm by solving the following problem:

$$\begin{array}{ll} \min & \max(|\tau_1|, |\tau_2|, |\tau_3|) \\ \text{s.t.} & T_1 = \tau_1 + \tau_3 \\ & T_2 = \tau_2 + \tau_3 \end{array} \tag{10}$$

The solution in a closed form is expressed by three linear piecewise functions continuous in all the domain $D = (T_1, T_2)$

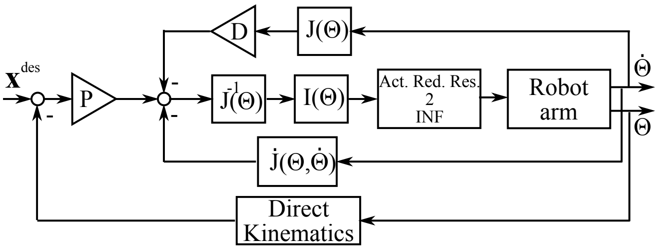

Fig. 3. Feedback position control with PD and linearization of robot arm inertia

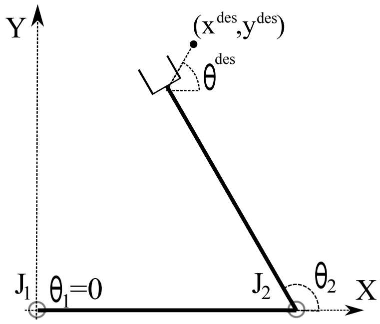

Fig. 4. Robot arm coordinate frame used in the simulation

[23]:

$$\tau_1 = \begin{cases} \frac{T_1 - T_2}{2} & \text{if } T_1T_2 \leq 0 \\ T_1 - \frac{T_2}{2} & \text{if } T_1T_2 > 0 \text{ and } |T_1| \leq |T_2| \\ \frac{T_1}{2} & \text{if } T_1T_2 > 0 \text{ and } |T_1| > |T_2| \end{cases} \quad (11)$$

$$\tau_2 = \begin{cases} \frac{T_2 - T_1}{2} & \text{if } T_1T_2 \leq 0 \\ \frac{T_2}{2} & \text{if } T_1T_2 > 0 \text{ and } |T_1| \leq |T_2| \\ T_2 - \frac{T_1}{2} & \text{if } T_1T_2 > 0 \text{ and } |T_1| > |T_2| \end{cases} \quad (12)$$

$$\tau_3 = \begin{cases} \frac{T_1 + T_2}{2} & \text{if } T_1T_2 \leq 0 \\ \frac{T_2}{2} & \text{if } T_1T_2 > 0 \text{ and } |T_1| \leq |T_2| \\ \frac{T_1}{2} & \text{if } T_1T_2 > 0 \text{ and } |T_1| > |T_2| \end{cases} \quad (13)$$

In this work, it is assumed that all the maximum joint actuator torques are the same (i.e. $\tau_1^{max} = \tau_2^{max} = \tau_3^{max}$). A solution for $\tau_1^{max} \neq \tau_2^{max} \neq \tau_3^{max}$ for both the 2 and infinity norm based approaches is available in [29].

V. SIMULATION DESCRIPTION AND ANALYSIS METHOD

The dynamics of a two-link planar robot arm actuated by one bi- and two mono-articular actuators are simulated. A position feedback controller with linearization of the robot arm inertia is designed in the operational space as illustrated in Fig. 3, where $I(q)$ is the robot arm inertia matrix. Friction is not taken into account, nor in the controller, nor in the robot arm dynamics. The actuator redundancy resolution approach in here is the same used under statics conditions ((7),(8), and (9) for 2 norm, while (11), (12), and (13) for infinity norm).

In Fig. 4 the robot arm coordinate frame is shown. The end effector desired position $\boldsymbol{X}^{des}$ is defined as

$$\boldsymbol{X}^{des} = \begin{bmatrix} x^{des} \\ y^{des} \end{bmatrix} = \begin{bmatrix} x^{ini} + dist\cos(\theta^{des}) \\ y^{ini} + dist\sin(\theta^{des}) \end{bmatrix}, \quad (14)$$

where x^{ini} and x^{ini} are the end effector initial position; $dist$ and θ^{des} are the desired end effector position magnitude and direction, respectively.

The parameters used in the simulation are shown in Tab. I. P gain is designed so to have an end effector frequency response of 1 Hz to a position step input along $\theta^{des} = 45°$ with $dist$ = 0.01 m when $\boldsymbol{\theta} = [\theta_1, \theta_2]^T = [0°, 90°]^T$. D gain is designed to have a damping factor of $\sqrt{2}/2$. The desired position is given as a step command. The response of the robot arm is evaluated comparing 2 and infinity norm approaches for actuation redundancy resolution. The simulation is performed in two condition regarding joint actuator limitation:

TABLE I
SIMULATION PARAMETERS

Parameter	value
Length link 1 and 2	1 m
Mass 1 and 2	5 Kg
COM 1 and 2	0.5 m
Momentum of Inertia 1 and 2	1.67 Kg/m^2
P and D gains	39.5 and 8.9

- $actuator_{lim}$=1: no limitation on maximum joint actuator torque (i.e. τ^{max}=max(τ_1, τ_2, τ_3)=∞).
- $actuator_{lim}$=2: the joint actuator torque is limited to the value obtained when using infinity norm (i.e. τ^{max}=max(τ_1, τ_2, τ_3) when using infinity norm).

Two factors are calculated, the ratio of maximum actuator joint torques (τ_{ratio}) and the ratio of maximum end effector acceleration acc_{ratio}. The value of τ_{ratio} is calculated when $actuator_{lim}$=1 as:

$$\tau_{ratio} = \frac{\max(|\tau_{1(\text{inf})}|, |\tau_{2(\text{inf})}|, |\tau_{3(\text{inf})}|)}{\max(|\tau_{1(2)}|, |\tau_{2(2)}|, |\tau_{3(2)}|)} = \frac{\tau_{(\text{inf})}^{max}}{\tau_{(2)}^{max}} \quad (15)$$

The ratio of maximum end effector acceleration acc_{ratio} is calculated in $actuator_{lim}$=2 as:

$$acc_{ratio} = \frac{|acc|_{(\text{inf})}^{max}}{|acc|_{(2)}^{max}}, \quad (16)$$

where $|acc|_{(\text{inf})}^{max}$ is the maximum magnitude of the acceleration during the robot arm movement.

The joint actuator torque saturation in $actuator_{lim}$=2 is implemented as:

j=0;
while (($\tau_i > \tau^{max}$ or $\tau_i < -\tau^{max}$) for $i = 1, 2, 3$) do
  $\boldsymbol{T}^{inp} = \boldsymbol{T}^{inp}(1 - 0.001j)$
  $j = j + 1$
end

where the actuators torque inputs $\boldsymbol{T}^{inp}$ are defined in respect to the actual position $\boldsymbol{X}^{act} = [x^{act}, y^{act}]^T$ as:

$$\boldsymbol{T}^{inp} = \boldsymbol{I}(\boldsymbol{\theta})\boldsymbol{J}(\boldsymbol{\theta})^{-1}\left(P(\boldsymbol{X}^{des} - \boldsymbol{X}^{act}) - D\dot{\boldsymbol{X}}^{act} - \dot{\boldsymbol{J}}(\boldsymbol{\theta}, \dot{\boldsymbol{\theta}})\dot{\boldsymbol{\theta}}\right) \quad (17)$$

Simulation is performed varying θ^{des} from 0 to 360° in increments of 0.1°, while the desired distance is constant, $dist = 0.01$ m.

VI. RESULTS

At first, the response to a position step input of the robot arm in the initial position $\boldsymbol{\theta} = [0, 90°]^T$, a desired end effector position with $dist = 0.01$, and $\theta^{des} = 0°$ is shown for $actuator_{lim}$=(1,2). Then, τ_{ratio} and acc_{ratio} are shown in respect to θ^{des} for three configuration.

A. Time response for $\boldsymbol{\theta} = [0, 90°]^T$ and $\theta^{des} = 0°$

The end effector position and the actuator joint torques of the robot arm in the initial position $\boldsymbol{\theta} = [0, 90°]^T$, and a desired end effector position with $dist = 0.01$ and $\theta^{des} = 0°$, are illustrated in Fig. 5 for $actuator_{lim}$=1. The end effector position, as well the joint torques, are the same for both 2 and infinity norms. However, the joint actuator torques differs in the two cases: $\tau^{max}_{(2)} = \tau_{3(2)} = 0.7681$ Nm and $\tau^{max}_{(\text{inf})} = \tau_{3(\text{inf})} = 0.5760$ Nm, therefore $\tau_{ratio} = 0.75$.

In Fig. 6 the joint torques, actuator joint torques, and acceleration magnitude of the end effector when $actuator_{lim}$=2 are shown in Fig. 6 The maximum joint actuator torques is limited, $\tau^{max} = \tau_{3^{max}(\text{inf})} = \tau^{max}_{\text{inf}} = 0.5760$ Nm. The magnitude of end effector acceleration differs for the 2 and infinity norm: $|acc|^{max}_{(\text{inf})}$=0.3941 m/s^2 and $|acc|^{max}_{(2)}$=0.2964 m/s^2, therefore $acc_{ratio} = 1.33$.

B. τ_{ratio} and acc_{ratio} in respect to θ^{des}

In Fig. 7, the values of τ_{ratio} and acc_{ratio} are shown in respect to the end effector desired position direction $\theta^{des} \in [0, 360°]$ for three arm configurations: $\boldsymbol{\theta} = [0, 30°]^T$, $\boldsymbol{\theta} = [0, 90°]^T$, and $\boldsymbol{\theta} = [0, 150°]^T$. Detailed explanation is provided in Section VII.

VII. DISCUSSION

From the simulation and results analysis the following is deduced.

Given the same robot arm dynamics the infinity norm approach requires a maximum joint actuator torque lower than the one required by the 2 norm approach (from Fig. 5(c) and Fig. 7).

For the same maximum joint actuator torques, the infinity norm approach produces higher end effector acceleration magnitude (from Fig. 6(c) and Fig. 7).

The value of τ_{ratio} is equal to the reciprocal of acc_{ratio}. When $actuator_{lim}$=2 and at least one actuator joint desired torque is greater than the maximum one, both the desired actuator torque inputs $\boldsymbol{T}^{inp}$ are reduced by the same value in proportion to their magnitude. The end effector virtual force, defined as

$$\boldsymbol{F}^{vir} = \left(\boldsymbol{J}(\boldsymbol{\theta})^T\right)^{-1} \boldsymbol{T}^{inp} \tag{18}$$

has therefore the same direction as the desired one, while its magnitude is reduced proportionally to the reduction in actuator joint torque. The end effector acceleration magnitude is directly proportional to the virtual force magnitude. Therefore, the force ratio $virfor_{ratio} = \boldsymbol{F}^{vir}_{(\text{inf})} / \boldsymbol{F}^{vir}_{(2)}$ is equal

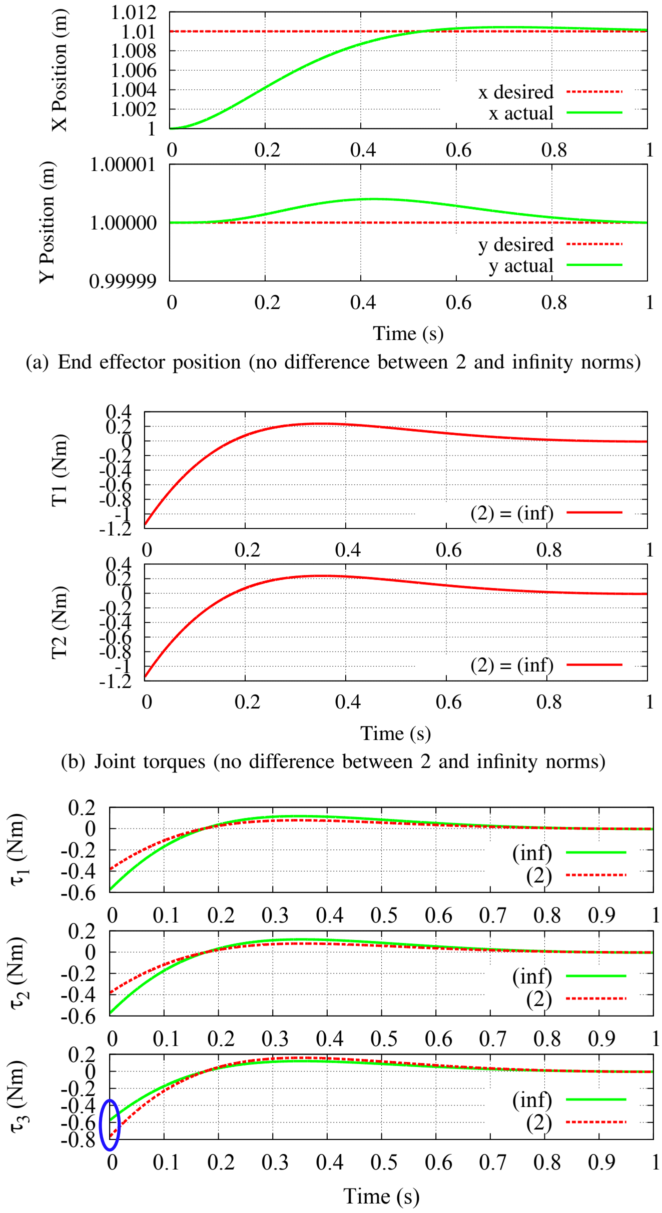

(a) End effector position (no difference between 2 and infinity norms)

(b) Joint torques (no difference between 2 and infinity norms)

(c) Actuator joint torques (2 norm needs greater maximum actuator joint torques)

Fig. 5. $actuator_{lim}$=1 ($\tau^{max} = \infty$): position step response for $\boldsymbol{\theta} = [0°, 90°]^T$, $\theta^{des} = 0°$

to acc_{ratio}. Given (15) and (16), it straightforward follows $\tau_{ratio} = (acc_{ratio})^{-1}$.

The values of both τ_{ratio} and acc_{ratio} do not depend on the feedback gains and $dist$ values. This is due to the fact that $acc_{ratio} = (\tau_{ratio})^{-1} = virfor_{ratio}$, and that the value of the gains and $dist$ appear in both numerator and denominator of $virfor_{ratio}$.

The value of τ_{ratio} is a function of robot arm configuration, inertia, and θ^{des}. There are six values of θ^{des} (a, b, c, d, e, f) in which $\tau_{ratio} = 1$ (i.e. 2 and infinity norm perform the same) and six values (A, B, C, D, E, F) in which $\tau_{ratio} = 0.75$ (i.e. the advantage of infinity norm is the highest). If the

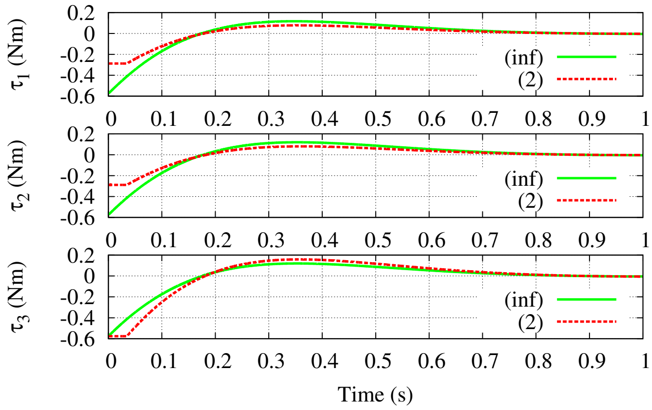

(a) Actuator joint torques (maximum actuator joint torque is the same for 2 and infinity norm)

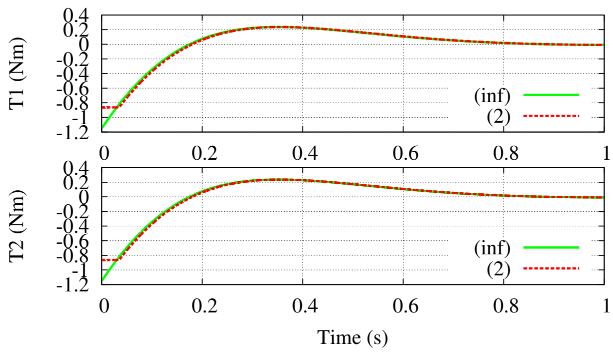

(b) Joint torques

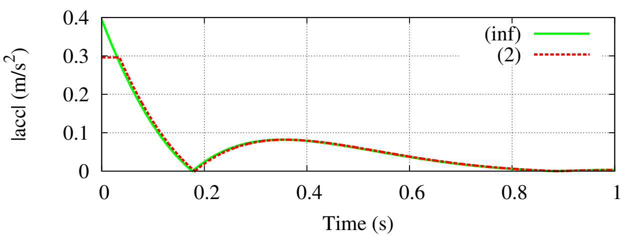

(c) Acceleration magnitude (greater for infinity norm)

Fig. 6. Actuator joint torques, joint torques, and acceleration magnitude for $actuator_{lim}$=2 ($\tau^{max} = \tau^{max}_{\text{inf}} = 0.5760$ Nm), $\boldsymbol{\theta} = [0°, 90°]^T$, $\theta^{des} = 0°$

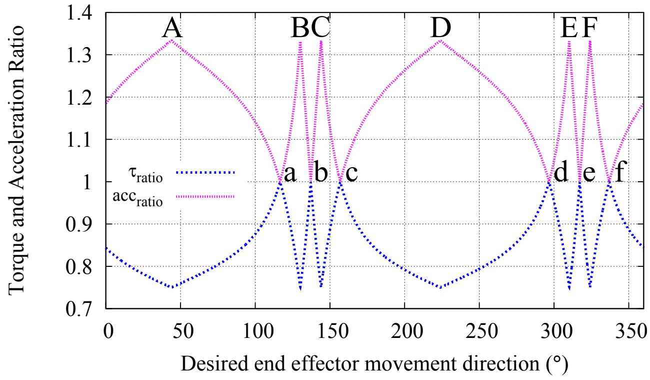

(a) $\boldsymbol{\theta} = [0, 30°]^T$

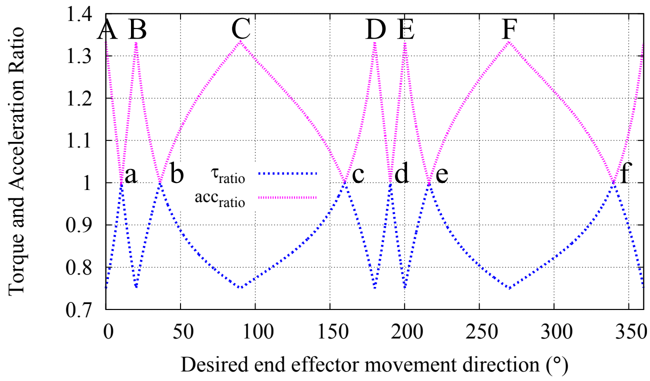

(b) $\boldsymbol{\theta} = [0, 90°]^T$

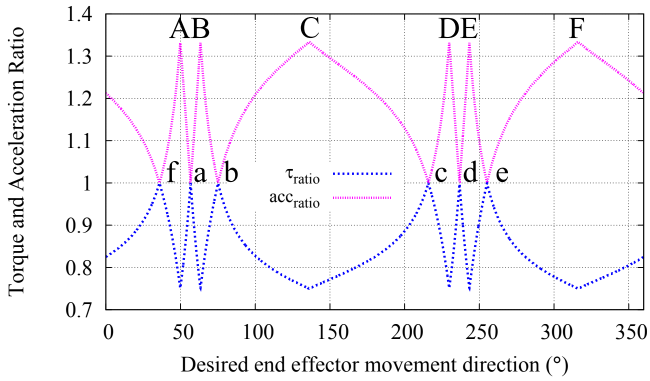

(c) $\boldsymbol{\theta} = [0, 150°]^T$

Fig. 7. Torque (τ_{ratio}) and acceleration (acc_{ratio}) ratios

three maximum joint actuator torques are the same (i.e. $\tau_1^{max} = \tau_2^{max} = \tau_3^{max}$), θ^{des} of points A, B, C, D, E, F results when joint torques are same ($T_1 = T_2$), or one of the two is null ($T_1 = 0$ or $T_2 = 0$), as shown in Tab. II. The cases illustrated in Tab. II are derived from the analysis of matrix $\boldsymbol{B}$, the equations of the 2 norm approach ((7),(8), and (9)), and the ones of infinity norm approach ((11), (12), and (13)). For example, considering the case $T_1 = T_2 = 1$ Nm, using the 2 norm approach $\boldsymbol{\tau} = [0.33, 0.33, 0.67]^T$, while using infinity norm approach $\boldsymbol{\tau} = [0.5, 0.5, 0.5]^T$. Therefore $\tau_{ratio} = 0.75$. It is trivial to verify that $\tau_{ratio} = 0.75$ also in the other five cases (B, C, D, E, F). This explains why the minimum values for τ_{ratio} is 0.75 in all the 6 cases. For the controller in Fig. 4 the relationship between desired end effector position and joint torques is (17). By setting the joint torques as in Tab. II in (17), θ^{des} of points A, B, C, D, E, F is calculated.

The analytical function of τ_{ratio} for any given robot arm configuration is calculated using (17) together with Tab. II, the 2 norm approach equations ((7), (8), and (9)), and the infinity norm approach equations ((11), (12), and (13)). For example, between point A and a, from Tab. II and (7), (8), (9), (11), (12), and (13) follows that the maximum actuator joint torque is τ_3 for both norms, τ_{ratio} is therefore given by:

$$\tau_{ratio} = \frac{|\tau_{3(\text{inf})}|}{|\tau_{3(2)}|} = \frac{1.5|T_1|}{|T_1 + T_2|} \tag{19}$$

The values of T_1 and T_2 in (19) are expressed by (17). Similarly, the analytical expression for τ_{ratio} is obtained for the other cases.

Under static condition, or for a position feedback con-

TABLE II

RELATION BETWEEN θ^{des} DIRECTIONS (A,B,C,D,E,F) AND (a,b,c,d,e,f) AND JOINT TORQUES

A	$T_1 = T_2$ and $T_1 < 0$	a	$2T_1 = T_2$ and $T_1 < 0$
B	$T_1 = 0$ and $T_2 < 0$	b	$T_1 = -T_2$ and $T_1 > 0$
C	$T_1 > 0$ and $T_2 = 0$	c	$T_1 = 2T_2$ and $T_1 > 0$
D	$T_1 = T_2$ and $T_1 > 0$	d	$2T_1 = T_2$ and $T_1 > 0$
E	$T_1 = 0$ and $T_2 > 0$	a	$T_1 = -T_2$ and $T_1 < 0$
F	$T_1 < 0$ and $T_2 = 0$	e	$T_1 = 2T_2$ and $T_1 < 0$

trol without robot arm inertia linearization, θ^{des} of points A,B,C,D,E,F depends only on the robot arm Jacobian, as in (4). If $\tau_1^{max} \neq \tau_2^{max} \neq \tau_3^{max}$, the joint torques conditions in Tab. II vary, as well the minimum value of τ_{ratio}. However, using the same procedure shown here, it is possible to determine the analytical expression for τ_{ratio}.

VIII. CONCLUSIONS

The proposed infinity norm approach with closed form solution to resolve actuator redundancy for bi-articularly actuated robot arms is compared with the 2 norm based approach under dynamic conditions, by simulation means.

From the quantitative analysis we conclude that infinity norm approach in respect to the 2 norm approach:

- Given a desired end effector position, reduces the required maximum joint actuator torque up to 25%
- Given the maximum joint actuator torques, increases the achievable maximum end effector acceleration magnitude (or virtual force magnitude) up to 33%

In addition, the analytical relationship between these two advantages and the parameters on which they depend — robot arm configuration, inertia matrix, and end effector desired movement direction — is provided.

REFERENCES

[1] N. Hogan, "Impedance control: An approach to manipulation: Part III—Applications," *Journal of Dynamic Systems, Measurement, and Control*, vol. 107, no. 1, pp. 17–24, Mar. 1985.

[2] T. Horita, P. V. Komi, C. Nicol, and H. Kyrlinen, "Interaction between pre-landing activities and stiffness regulation of the knee joint musculoskeletal system in the drop jump: implications to performance," *European Jour. of Appl. Physiology*, vol. 88, no. 1-2, pp. 76–84, 2002.

[3] S. Oh, Y. Kimura, and Y. Hori, "Reaction force control of robot manipulator based on biarticular muscle viscoelasticity control," in *Advanced Intelligent Mechatronics (AIM)*, 2010, pp. 1105–1110.

[4] G. J. Van Ingen Schenau, "From rotation to translation: Constraints on multi-joint movements and the unique action of bi-articular muscles," *Human Movement Science*, vol. 8, no. 4, pp. 301–337, Aug. 1989.

[5] K. Hosoda, Y. Sakaguchi, H. Takayama, and T. Takuma, "Pneumatic-driven jumping robot with anthropomorphic muscular skeleton structure," *Autonomous Robots*, vol. 28, no. 3, pp. 307–316, Dec. 2009.

[6] M. A. Lewis, M. R. Bunting, B. Salemi, and H. Hoffmann, "Toward ultra high speed locomotors: Design and test of a cheetah robot hind limb," in *IEEE International Conference on Robotics and Automation (ICRA)*, 2011.

[7] T. Oshima, N. Momose, K. Koyanagi, T. Matsuno, and T. Fujikawa, "Jumping mechanism imitating vertebrate by the mechanical function of bi-articular muscle," in *Mechatronics and Automation, 2007. ICMA 2007. International Conference on*, 2007, pp. 1920–1925.

[8] R. Niiyama, S. Nishikawa, and Y. Kuniyoshi, "Athlete robot with applied human muscle activation patterns for bipedal running," in *International Conference on Humanoid Robots*, 2010, pp. 498–503.

[9] K. Tadano, M. Akai, K. Kadota, and K. Kawashima, "Development of grip amplified glove using bi-articular mechanism with pneumatic artificial rubber muscle," in *2010 IEEE International Conference on Robotics and Automation (ICRA)*, May 2010, pp. 2363–2368.

[10] V. Salvucci, S. Oh, Y. Hori, and Y. Kimura, "Disturbance rejection improvement in non-redundant robot arms using bi-articular actuators," in *Intern. Symp. on Industrial Electronics (ISIE)*, 2011, pp. 2159–2164.

[11] T. Fujikawa, T. Oshima, M. Kumamoto, and N. Yokoi, "Output force at the endpoint in human upper extremities and coordinating activities of each antagonistic pairs of muscles." *Transactions of the Japan Society of Mechanical Engineers. C*, vol. 65, no. 632, pp. 1557–1564, 1999.

[12] Y. Nakata, A. Ide, Y. Nakamura, K. Hirata, and H. Ishiguro, "Hopping of a monopedal robot with a biarticular muscle driven by electromagnetic linear actuators," in *2012 IEEE International Conference on Robotics and Automation (ICRA)*, May 2012, pp. 3153 –3160.

[13] T. Tsuji, "A model of antagonistic triarticular muscle mechanism for lancelet robot," in *2010 11th IEEE International Workshop on Advanced Motion Control*. IEEE, Mar. 2010, pp. 496–501.

[14] K. Yoshida, N. Hata, S. Oh, and Y. Hori, "Extended manipulability measure and application for robot arm equipped with bi-articular driving mechanism," in *Industrial Electronics, 2009. IECON '09. 35th Annual Conference of IEEE*, 2009, pp. 3083–3088.

[15] Y. Kimura, S. Oh, and Y. Hori, "Novel robot arm with bi-articular driving system using a planetary gear system and disturbance observer," in *Advanced Motion Control, 2010 11th IEEE International Workshop on*, 2010, pp. 296–301.

[16] M. Shinohara, A. Umemura, T. Haneyoshi, and Y. Saito, "Coordination control of bi-articular robotic arm by motor drive with planetary gear," in *International Power Electronics Conference*, 2010, pp. 2551–2556.

[17] V. Salvucci, Y. Kimura, S. Oh, and Y. Hori, "BiWi: bi-articularly actuated and wire driven robot arm," in *IEEE International Conference on Mechatronics (ICM)*, Apr. 2011, pp. 827–832.

[18] M. A. Lewis and T. J. Klein, "Achilles: A robot with realistic legs," in *IEEE Biomedical Circuits and Systems Conference (BIOCAS)*, 2008.

[19] A. Seyfarth, F. Iida, R. Tausch, M. Stelzer, O. von Stryk, and A. Karguth, "Towards bipedal jogging as a natural result of optimizing walking speed for passively compliant Three-Segmented legs," *Intern. Journal of Robotics Research*, vol. 28, no. 2, pp. 257 –265, 2009.

[20] A. Z. Shukor and Y. Fujimoto, "Modelling and control of redundant robot manipulator using spiral motor," in *6th Europe-Asia Congress on Mechatronics EAM, Proceedings of*, 2010, pp. 59–65.

[21] C. A. Klein and C. H. Huang, "Review of pseudoinverse control for use with kinematically redundant manipulators," *IEEE Transactions on Systems, Man, and Cybernetics*, vol. 13, pp. 245–250, 1983.

[22] V. Salvucci, S. Oh, and Y. Hori, "Infinity norm approach for precise force control of manipulators driven by bi-articular actuators," in *IECON 2010 - 36th Annual Conference on IEEE Industrial Electronics Society*, Nov. 2010, pp. 1908–1913.

[23] V. Salvucci, Y. Kimura, S. Oh, and Y. Hori, "Experimental verification of infinity norm approach for force maximization of manipulators driven by bi-articular actuators," in *American Control Conference (ACC)*, 2011.

[24] V. Salvucci, Y. Kimura, S. Oh, T. Koseki, and Y. Hori, "Comparing approaches for actuator redundancy resolution in bi-articularly actuated robot arms," *Mechatronics, IEEE/ASME Transactions on*, May 2013.

[25] V. Salvucci, Y. Kimura, S. Oh, and Y. Hori, "Non-linear phase different control for precise output force of bi-articularly actuated manipulators," *Advanced Robotics*, vol. 27, no. 2, pp. 109–120, 2013.

[26] H. Fukusho, T. Sugimoto, and T. Koseki, "Control of a straight line motion for a two-link robot arm using coordinate transform of bi-articular simultaneous drive," in *Advanced Motion Control, 2010 11th IEEE International Workshop on*, 2010, pp. 786–791.

[27] M. Kumamoto, T. Oshima, and T. Yamamoto, "Control properties induced by the existence of antagonistic pairs of bi-articular muscles – mechanical engineering model analyses," *Human Movement Science*, vol. 13, no. 5, pp. 611–634, Oct. 1994.

[28] S. Oh, V. Salvucci, and Y. Hori, "Development of simplified statics of robot manipulator and optimized muscle torque distribution based on the statics," in *American Control Conference (ACC)*, July 2011, pp. 4099–4104.

[29] V. Salvucci, Y. Kimura, S. Oh, and Y. Hori, "Force maximization of biarticularly actuated manipulators using infinity norm," *IEEE/ASME Transactions on Mechatronics*, vol. 18, no. 3, pp. 1080–1089, June 2013.